Evidence of Reactive Aromatics As a Major Source of Peroxy Acetyl Nitrate over China

ZHEN LIU,*,† YUHANG WANG,† DASA GU,† CHUN ZHAO,†,‡ L. GREGORY HUEY,† ROBERT STICKEL,† JIN LIAO,† MIN SHAO,§ TONG ZHU,§ LIMIN ZENG,§ SHAW-CHEN LIU,|| CHIH-CHUNG CHANG,|| ANTONIO AMOROSO,⊥ AND FRANCESCA COSTABILE⊥

School of Earth and Atmospheric Sciences, Georgia Institute of Technology, Atlanta, Georgia, College of Environmental Sciences and Engineering, Peking University, Beijing, China, Research Center for Environmental Changes (RCEC), Academic Sinica, Taipei, China, and Institute for Atmospheric Pollution, National Research Council (CNR-IIA), Rome, Italy

Received March 12, 2010. Revised manuscript received July 28, 2010. Accepted July 30, 2010.

We analyze the observations of near-surface peroxy acetyl nitrate (PAN) and its precursors in Beijing, China in August of 2007. The levels of PAN are remarkably high (up to 14 ppbv), surpassing those measured over other urban regions in recent years. Analyses employing a 1-D version of a chemical transport model (Regional chEmical and trAnsport Model, REAM) indicate that aromatic non-methane hydrocarbons (NMHCs) are the dominant (55−75%) PAN source. The major oxidation product of aromatics that produces acetyl peroxy radicals is methylglyoxal (MGLY). PAN and O_3 in the observations are correlated at daytime; aromatic NMHCs appear to play an important role in O_3 photochemistry. Previous NMHC measurements indicate the presence of reactive aromatics at high levels over broad polluted regions of China. Aromatics are often ignored in global and (to a lesser degree) regional 3D photochemical transport models; their emissions over China as well as photochemistry are quite uncertain. Our findings suggest that critical assessments of aromatics emissions and chemistry (such as the yields of MGLY) are necessary to understand and assess ozone photochemistry and regional pollution export in China.

Introduction

PAN ($CH_3C(O)OONO_2$) is one of the major components of photochemical smog as well as an important player in atmospheric chemistry. It is formed by the reaction between acetyl peroxy (PA) radical ($CH_3C(O)OO$) and nitrogen dioxide (NO_2) and is removed mainly via thermal decomposition near the surface, with its lifetime ranging from less than one to several hours depending on the ambient temperature and the NO/NO_2 ratio (*1*). PA radical comes from photolysis or OH oxidation of a number of oxygenated volatile organic compounds (OVOCs), such as acetaldehyde (CH_3CHO), acetone (CH_3COCH_3), methyl vinyl ketone (MVK, CH_2-$CHC(O)CH_3$), methacrolein (MACR, CH_2CCH_3CHO), methylglyoxal (MGLY, $CH_3C(O)CHO$), and biacetyl ($CH_3C(O)$-$C(O)CH_3$) (*2*), which either form in situ by oxidation of various nonmethane hydrocarbons (NMHCs) or are emitted from primary sources (e.g., acetaldehyde). The relative importance of PA radical precursors is highly variable depending on the composition of the NMHC and NO_x ($NO + NO_2$) mix (*2, 3*). While acetaldehyde is often the dominant PA radical source over urban regions (*4, 5*), isoprene oxidation products, e.g. MVK, MACR, and MGLY, usually play an important role over regions with significant biogenic emissions (*1, 2*). Occasionally, OVOCs from aromatics and alkenes could be more important than acetaldehyde over some urban regions (*6*). Due to the much shorter lifetime of PAN than that of O_3 in the boundary layer, in situ measurements provide considerably better constraints for PAN chemistry than for O_3 chemistry, and analyzing PAN sources can provide insights into formation mechanisms of photochemical pollution.

Photochemical pollution has become an important air quality issue in China, due to increased emissions of NO_x and volatile organic compounds (VOCs) driven by the rapid economic growth. Remarkably elevated O_3 levels have been found at both local (*7*) and regional (*8*) scales. While more measurements of O_3 and its precursors become available (*9*−*11*), more detailed modeling analysis of the photochemistry and transport is desirable (*12, 13*).

PAN has been measured in many urban and suburban regions across the world (*1, 2, 4*−*6, 14, 15*). To our knowledge, PAN measurements and analysis of PAN photochemsitry in China are still sparse. Up to 10 ppbv of PAN has been observed at an urban site (the same site as ours) of Beijing (*11*). Elevated PAN levels (up to 9 ppbv) have also been measured at a suburban site of Lanzhou in the western part of China, accompanied by moderate PAN levels (0.44 ± 0.16 ppbv) at a downwind remote site of Wuliguan, which was suggested to be mainly due to transport from Lanzhou (*16*). Recently, measurements of peroxyacetic acid in China were reported, and aromatics were identified as the major source (45%) of peroxyacetic acid (*17*).

In this work, we employ the 1-D version of a CTM (Regional chEmical and trAnsport Model, REAM) to analyze in situ measurements of a full suite of pollutants in Beijing, China, focusing on both photochemical and transport sources of PAN.

Methods

Measurements. Within the framework of the Campaign of Air Quality Research in Beijing 2007 (CAREBeijing-2007), a full suite of trace gases were measured simultaneously at an urban site in Beijing in August 2007. The site is located on a building roof top (~20 m above the ground level) on the campus of Peking University (39.99°N, 116.31°E). Nitrogen monoxide (NO) was measured with a custom-made chemiluminescence detector (*18*). Total reactive nitrogen compounds (NO_y, only gas phase) were measured by the conversion of the NO_y species to NO on a molybdenum converter operated at 300 °C. Laboratory tests show that the conversion efficiency for NO_2 and HNO_3 is measured to be larger than 95% and 85%, respectively. PAN was measured using a chemical ionization mass spectrometer (CIMS) (*19*). HONO was measured with a liquid coil scrubbing/UV−vis

* Corresponding author phone: (404)825-7319; e-mail: zhen.liu@eas.gatech.edu.
† Georgia Institute of Technology.
‡ Present address: The Pacific Northwest National Laboratory, Richland, Washington.
§ Peking University.
|| Academic Sinica.
⊥ National Research Council (CNR-IIA).

10.1021/es1007966 © 2010 American Chemical Society
Published on Web 08/16/2010

instrument (*20*). Under summer conditions at Beijing, interferences during sampling on the order of 2−9% of the measured HONO mixing ratios were observed and corrected using sodium carbonate denuders (Supporting Information) (*21, 22*). O_3 and CO were measured by commercial instruments from the ECOTECH (EC9810 and EC9830). C_3−C_9 NMHCs were measured with a time resolution of 30 min using two online GC-FID/PID systems (Syntech Spectra GC-FID/PID GC955 series 600/800 VOC analyzer), one for the C_3−C_5 NMHCs, and the other for C_6−C_9 NMHCs (*11*). Another automated GC/MS/FID system was deployed to measure NMHCs at daytime (8:00−9:00 and 13:00−14:00) (*12*). OVOCs were measured using the PFPH-GC/MS method (*23*). The uncertainties (one standard deviation) for these measurements are estimated to be 5% for NO, O_3, CO, 3%−5% for NMHCs, 10% for NO_y, PAN, HONO, and OVOCs. More detailed descriptions of the instruments and experimental methods are available in the Supporting Information.

1-D REAM Model. Previously, we have applied the 3-D Regional chEmical and trAnsport Model (REAM) to investigate O_3 photochemistry and transport at north mid latitudes (*24*−*30*). In this work, the 1-D version of the REAM model (1-D REAM), including the modules for O_3−NO_x-hydrocarbon photochemistry, diffusion and convective transport, and wet/dry deposition, was used for analyzing the measurements in Beijing. The kinetic data were updated with the latest compilation (*31*). The NMHC chemistry is expanded by including chemistry of aromatics based on the SAPRC-07 chemical mechanism (Supporting Information) (*32*). Transport is simulated using the WRF assimilated meteorological fields based on the NCEP reanalysis data (Supporting Information) (*29*). In order to simulate PAN, the model is constrained with measured CO, O_3, NO, HONO, NMHCs (C_2−C_9), and OVOCs (acetone, acetaldehyde, and formaldehyde) at every 1-min time step. Free radicals and other OVOC species that are also important in PAN chemistry but were not measured, such as MVK, MACR, MGLY, and biacetyl, are simulated in the model, and we note that measurements of all these intermediates would further improve this type of study. We ran the model continuously from August 1 to 30, 2007, and results for the last 20 days were analyzed because PAN measurements are available for the last 20 days of the measurement period.

Results and Discussions

Observed Elevated PAN Levels. The mean diurnal profiles of measured PAN, O_3, NO_y, NO, and HONO during August 10 to 30, 2007 are shown in Figure 1. The mean daily maximum PAN mixing ratio is 5 ppbv, occurring in the afternoon around 15:00, and the maximum during the measurement period reaches as high as 14 ppbv. Such abundance of PAN is comparable with that in Los Angeles during the late 1980s (*14*) and among the highest records in the past decade (*1, 2, 4*−*6, 15, 33*). The lifetime of PAN (calculated based on simulated PAN concentrations and loss reaction rates) is very short at daytime (~0.5 h), mainly due to high temperature at the surface (28 °C−38 °C) and a relatively large NO/NO_2 ratio (~0.5), which facilitate thermal decomposition of PAN and removal of PA radicals, respectively. Therefore, the large abundance of PAN at daytime indicates a large source of PA radicals from VOC oxidation and very fast photochemical processing in Beijing.

Also notable are the observed high nighttime PAN levels (1−2 ppbv), which are among the highest in the published literature (*15, 16, 33*). After inspecting measurements from previous studies and this experiment, we found that the ratio of nighttime average to daytime peak value, i.e. 1.5 ppbv/5 ppbv in this work lies in the range of 0.2−0.35 of previous measurements, e.g. 1 ppbv/5 ppbv for Mexico City (*15*), 0.45 ppbv/2 ppbv for Lanzhou of China (*16*), and 0.29 ppbv/0.91 ppbv for Houston (*33*), suggesting that the nighttime PAN levels are associated with the corresponding daytime magnitudes. The relatively long lifetime of PAN (2−5 h) due to low temperature (e.g., 21 °C−28 °C during our measurements) and a larger NO_2/NO ratio and shallow mixing layer are the two main factors leading to the continuous presence of PAN at night.

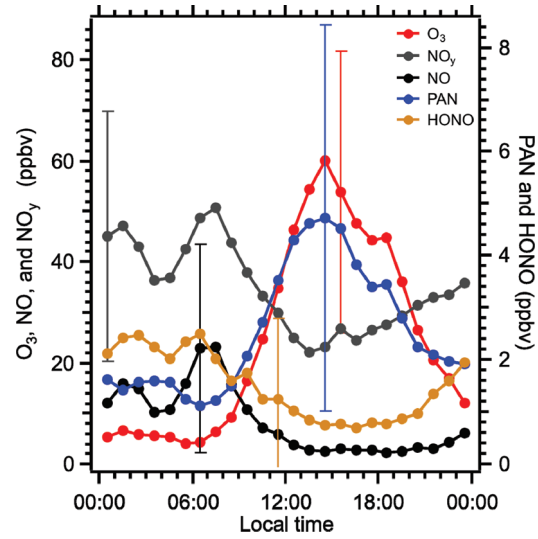

FIGURE 1. Average hourly diurnal profiles for measured O_3, NO_y, and its components during August 10−30, 2007, including NO, HONO, and PAN, together with corresponding standard deviations (only the largest hourly standard deviation for each species is shown).

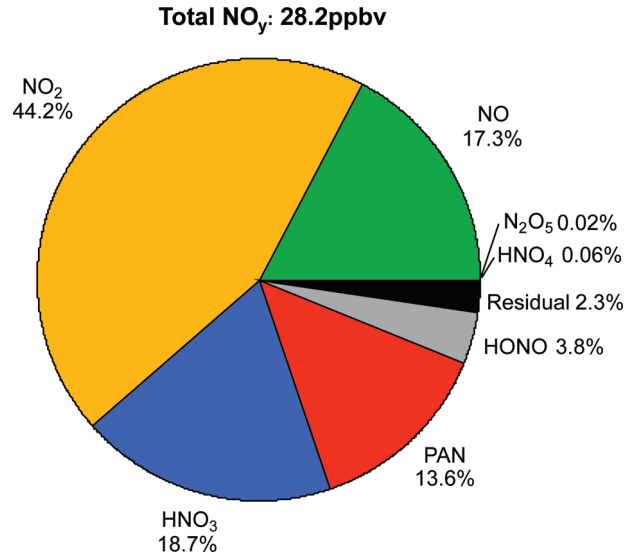

FIGURE 2. Average daytime (9:00−18:00) NO_y budget during August 10−30, 2007, in which NO, NO_y, PAN, and HONO are measured, and the other species (not directly measured) are from the 1-D model simulation (full aromatics). Residual denotes the difference between measured NO_y and the sum of measured and simulated NO_y components.

Daytime NO_y Budget. We examined the closure of NO_y budget at daytime when photochemistry is active. Average daytime (9:00−18:00) NO_y budget comprised of measured (NO, PAN, HONO) and model predicted (NO_2, N_2O_5, HNO_4, and gaseous HNO_3) mixing ratios of NO_y species is shown in Figure 2. The budget is reasonably closed with ~2% NO_y not accounted for. Some of the error may lie in the model simulation of HNO_3, the lifetime of which is ~6 h (against deposition to surface), longer than the other reactive nitrogen species. NO_z ($[NO_z] = [NO_y] - [NO_x]$) species together

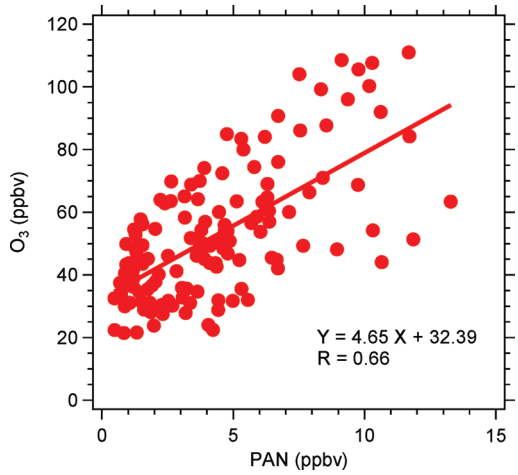

FIGURE 3. 1-h mean observed O_3 mixing ratios as a function of observed PAN for daytime (9:00−18:00) during August 10−30, 2007. Data points with O_3 larger than 20 ppbv are shown.

accounted for ~40% of total NO_y, consistent with a previous study in Beijing (*10*), suggesting the large abundance of oxidants from fast photochemical oxidation of NO_x. On average, PAN accounts for ~14% of total NO_y. From morning to afternoon, PAN percentage increases from ~5% to ~25% (Figure 1). It is also noteworthy that over 1 ppbv of HONO was observed at daytime (Figure 1), accounting for ~4% of the total NO_y (Figure 2). Such high levels of daytime HONO are significantly higher than other urban regions (*21*, *34*, *35*). Analyses of model results indicate that if assuming HONO is produced through heterogeneous processes (*36*, *37*), photolysis of HONO contributes to 25% of the average 24-h OH concentration and the majority (more than 60%) of the primary OH production rate throughout the daytime (unpublished results). The impact of HONO on PAN formation is also discussed in this paper.

The diurnal variations of PAN and O_3 tracks each other well, with their peaks at ~15:00 (Figure 1). Figure 3 shows good correlations of PAN and O_3 mixing ratios during daytime (9:00−18:00). The linear correlation between PAN and O_3 reflects that both species are products of NO_x and peroxy radicals. Thus, understanding the chemistry of PAN formation also facilitates the investigation of O_3 formation mechanism.

Chemical and Transport Sources of PAN. The original REAM photochemical mechanism is adopted from the GEOS-Chem model (*38*). Using this base version of the 1-D REAM model, we found that the model significantly underestimated PAN by a factor of 4 (Figure 4). In this simulation, the model is constrained by observed acetaldehyde and acetone, which are major sources of PA radical, and all the observed NMHCs except for aromatics. Although MGLY is also a major source of PA radical, there were few MGLY measurements available (August 15−20, 3-h resolution), so we did not use measured MGLY. We noticed that the simulated MGLY (less than 0.1 ppbv) concentrations are much lower than the observed values (0.9 ± 0.4 ppbv), indicating some important NMHCs as MGLY sources are missing in the model.

Inspection of the measurements of NMHCs shows that ~50% of observed NMHCs are aromatics (Figure S1 in the Supporting Information). Among fast-reacting NMHCs, toluene, xylenes, and ethylbenzene are among the group with the highest mixing ratios. A major oxidation product of these aromatic species is MGLY (Table S1 and Figure S1 in the Supporting Information). In subsequent simulations we expanded the photochemical mechanism in the model with chemistry of aromatic NMHCs based on the SAPRC-07 mechanism (*32*). The model predicted PAN values increase considerably, leading to better agreement with the measurements (Figure 4), but there is still on average ~25% of 24-h

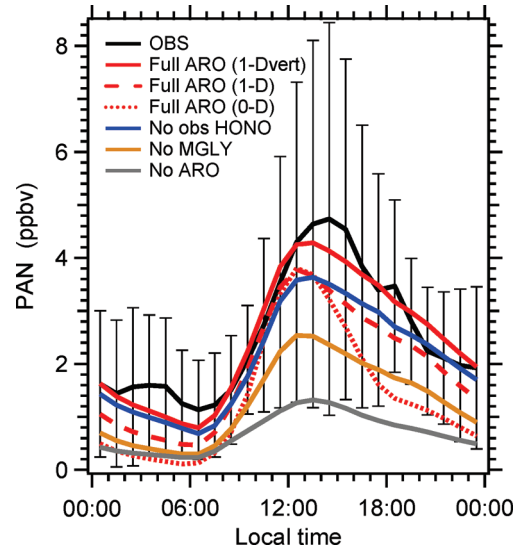

FIGURE 4. Average hourly diurnal profiles of measured PAN (black line) together with standard deviations (black bars) and model predicted PAN in different scenarios: (1) 1-D model incorporating a full aromatics-degradation mechanism (red solid line) using observed vertical profiles (*35*); (2) 1-D model incorporating a full aromatics-degradation mechanism (red dashed line) with only surface aromatics constrained by the observations; (3) a box model simulation incorporating a full aromatics-degradation mechanism (red dotted line); (4) 1-D model incorporating an aromatics-degradation mechanism, which does not include the production of MGLY (brown line), using the observed aromatic VOC vertical profiles (*35*); (5) 1-D model without surface HONO constrained by the measurements (blue line), using the observed aromatic VOC vertical profiles (*35*); (6) 1-D model without aromatics (gray line). "1-Dvert" and "1-D" denote with and without observed NMHC vertical profiles, respectively.

average PAN unexplained in the model (all relative changes are with respect to 24-h mean values hereafter).

In the two simulations mentioned above, the model is only constrained by surface observations since we did not have measurements at higher altitudes. Such a model configuration is equivalent to assuming that all the emission sources are located at the surface, and the trace gases in the boundary layer are all due to transport from surface by turbulent diffusion. By comparing with previous measurements in Beijing, we found that model simulated vertical gradients of aromatics are evidently larger than the measurements in a previous study (*39*). Although those measurements were at a different site in Beijing in the fall, it points to the possibility of large underestimates of aromatic NMHCs at 100−400 m in our model. One potential model bias is that WRF simulated eddy diffusion coefficients are too low, leading to overestimated vertical concentration gradient. Therefore, we conducted a sensitivity simulation by increasing the boundary layer eddy diffusion coefficients by a factor of 5, and the simulated vertical gradient of aromatics was still too large, which suggests that there are other reasons for underestimation of aromatics in the boundary layer, e.g. maybe there were some nonsurface sources of aromatics around the site. Coincidentally, previous studies found that in addition to vehicle emissions and solvent evaporations, several petrochemical plants located 10−30 km from our sampling site, e.g., Yanshan Petrochemical Plants in Fangshan, Beijing Chemical plants in Chaoyang, and Eastern Chemical Works in Tongzhou, are also major sources of aromatics at the observation site (*40*). It is likely that these nonsurface point sources at 100−200 m above the surface are responsible for the missing aromatics at 100−400 m in our model.

In a third simulation, by assuming there are nonsurface emissions of aromatics we further constrained our model at 20−400 m according to the observed vertical profiles of aromatics (*39*). Within our expectation, the model shows further improvements of simulated PAN from the previous results. The 1-D model reasonably reproduces the observed diurnal PAN profile, accounting for ∼95% of the measured values on average (Figure 4) as well as the day-to-day variation of PAN and most daytime peak values ($R = 0.71$, Figure S2 in the Supporting Information). Including profiles of other VOCs (such as alkenes) from the same study (*39*) in the model simulation does not significantly affect the model results. Detailed examination of the interaction between surface and boundary layer PAN production requires more measurements than available in this study and should be targeted in a future study at the measurement site.

Comparing the results of the third simulation to the second one shows that nonsurface aromatic NMHC emissions increased near-surface PAN concentrations by ∼20%. This result indicates the significant impact of downward transport of PAN produced aloft in the boundary layer on the measured PAN levels near the surface. In a previous study of PAN sources at Tokyo, Kondo et al. suggested that missing downward transport of PAN from the boundary layer is a main factor leading to the underestimation of PAN in their box model (*5*). They argued that the lower temperature at higher altitudes results in longer lifetimes and facilitates the downward transport of PAN to the surface. In order to investigate the contribution from downward transport, we ran the 1-D model as a box model by turning off the vertical transport. In this manner, the fraction of PAN produced at the surface layer and the rest transported from aloft to the surface can be isolated and compared with each other. Figure 4 shows that on average this box-model only explains about half of the measured PAN near surface, thereby suggesting that downward transport of PAN from aloft contributes the rest 50%. Our results are consistent with the previous study (*5*) and suggest that vertical mixing in the boundary layer is an important factor for generating elevated pollutant levels near the surface. Specifically with respect to PAN chemistry, downward transport has the direct effect of increasing PAN concentrations near the surface. Further, the decomposition of PAN transported from above provides a radical source and speeds up photochemical processing near the surface. For example, the 1-D model predicts 10% higher 24-h average OH concentration than the 0-D model.

We conducted a fourth sensitivity simulation to investigate the impact of MGLY on PAN formation. After removing the formation of MGLY in the model, simulated PAN concentrations drop by ∼50% (Figure 4), suggesting that half of the observed PAN concentrations are due to the production of MGLY during the oxidation of aromatics. The difference between the first (without aromatics, gray line) and the fourth (without MGLY, yellow line) simulations mainly reflects the contribution (∼20%) from another PAN precursor produced from aromatics - biacetyl. We further evaluated the contributions by each aromatic species to MGLY (and further to PAN) production based on their measured concentrations, reaction rate constants with OH and MGLY molar yields (Table S1 in the Supporting Information). The results show that m-xylene and 1,3,5-trimethylbenzene are the most efficient PAN precursors because of their relatively faster reaction rates with OH and larger MGLY yields (e.g., 64% for 1,3,5-trimethylbenzene), although their concentrations are only ∼20% and ∼4% of the most abundant aromatic species, toluene, respectively (Table S2 in the Supporting Information).

Based on the results of the above four simulations, we estimate that aromatics account for ∼75% of the total PAN source and MGLY from the oxidation of aromatics accounts for ∼50%. Most of MGLY (more than 90%) is produced by oxidation of aromatics. Considering the uncertainties introduced by using previously measured aromatics vertical profiles (*39*), the contribution of aromatics would lie in the range of 55−75% (by comparing PAN levels in "NO-ARO", "1-D", and "1-Dvert" simulations in Figure 4). The dominant role by aromatics is due to their larger proportion in the total NMHCs (∼50% in Figure S1) and faster production of PA radicals (through MGLY and biacetyl) than the other OVOCs. Contributions from the other major OVOCs are also obtained and tabulated in Table S3 in the Supporting Information.

Since PAN formation chemistry is initiated by reactions between NMHCs and OH, another necessity for maintaining the measured high PAN levels is a sufficient supply of OH. As mentioned above, our model analyses suggest that HONO serves as an important OH producer in Beijing (unpublished results), but current known HONO sources can only explain a small portion (∼0.1 ppbv) of the observed HONO (∼1 ppbv). We examined the impact from HONO on PAN formation chemistry by conducting a fifth sensitivity simulation in which we removed the observational constraint on HONO. Without fixing model HONO to the observed values, model predicted PAN concentrations drop considerably, by ∼15% on average and even more in the afternoon hours (Figure 4), underlining the important role of the abundant HONO (∼1 ppbv) during daytime as a major OH primary source for PAN formation.

Implications. Our finding that aromatics are the dominant (55−75%) source of PAN in Beijing is consistent with a recent study suggesting that aromatics account for ∼45% of the observed peroxyacetic acid (*17*). Previous studies reported comparable or even larger abundance of aromatic NMHCs over southern (*41, 42*) and eastern (*43*) China. Specifically, toluene has been found to be the main contributor to ozone formation in southern China (*41, 42*). Therefore, aromatics appear to be a major PAN (and O_3) precursor over polluted East China (*8*), in contrast to previous studies outside China indicating that alkenes and acetaldehyde are more important for PAN production (*4, 5*). However, aromatics are often ignored in global (*38, 44*) and (to a lesser degree) regional 3-D photochemical transport models (*45*); their emissions (*46*) over China as well as photochemistry (*32, 47*) are still quite uncertain. Ongoing modeling analysis (unpublished) reveals that regional anthropogenic emissions of aromatics are significantly underestimated over China. Our findings suggest that critical assessments of aromatics emissions and chemistry (such as the yields of MGLY) are necessary to understand and assess ozone photochemistry and export in China.

In addition, the comparison between a 1-D and box model simulation suggests that 1-D models may be more suitable than box models in analyzing in situ measurements of species such PAN, the lifetime of which changes drastically in the boundary layer. Downward transport of PAN from the boundary layer affects not only surface concentrations but also surface chemical reactivity by providing a source of radicals through decomposition. At polluted urban sites like Beijing, there is also evidence that nonsurface VOC and other precursor sources appear to be an important factor for surface concentrations of PAN via boundary layer-surface exchange.

Acknowledgments

This work was supported by the National Science Foundation Atmospheric Chemistry Program.

Note Added after ASAP Publication

The reference list and reference text citations were modified in the version of this paper published ASAP August 16, 2010. The correct version published on August 25, 2010.

Supporting Information Available

1) More detailed descriptions of instruments and experimental methods; 2) more detailed descriptions of the 1-D

REAM model the meteorological simulations in the 1-D version of REAM model; 3) estimation of model errors; 4) the aromatics oxidation mechanism used in the 1-D REAM model; 5) NMHC model input; and 6) 2 tables and 1 additional figure (Figure S1) mentioned in the text. This material is available free of charge via the Internet at http://pubs.acs.org.

Literature Cited

(1) Roberts, J. M.; Marchewka, M.; Bertman, S. B.; Sommariva, R.; Warneke, C.; de Gouw, J.; Kuster, W.; Goldan, P.; Williams, E.; Lerner, B. M.; Murphy, P.; Fehsenfeld, F. C. Measurements of PANs during the New England Air Quality Study 2002. *J. Geophys. Res.* **2007**, *112*, D20306, doi:10.1029/2007JD008667.

(2) LaFranchi, B. W.; Wolfe, G. M.; Thornton, J. A.; Harrold, S. A.; Browne, E. C.; Min, K. E.; Wooldridge, P. J.; Gilman, J. B.; Kuster, W. C.; Goldan, P. D.; de Gouw, J. A.; McKay, M.; Goldstein, A. H.; Ren, X.; Mao, J.; Cohen, R. C. Closing the peroxy acetyl nitrate budget: observations of acyl peroxy nitrates (PAN, PPN, and MPAN) during BEARPEX 2007. *Atmos. Chem. Phys.* **2009**, *9*, 7623–7641.

(3) Bowman, F. M.; Seinfeld, J. H. Ozone productivity of atmospheric organics. *J. Geophys. Res.* **1994**, *99*, 5309–5324.

(4) Roberts, J. M.; Stroud, C. A.; Jobson, B. T.; Tainer, M.; Hereid, D.; Williams, E.; Fehsenfeld, F.; Brune, W.; Martinez, M.; Harder, H. Application of a sequential reaction model to PANs and aldehyde measurements in two urban areas. *Geophys. Res. Lett.* **2001**, *28*, 4583–4586.

(5) Kondo, Y.; Morino, Y.; Fukuda, M.; Kanaya, Y.; Miyazaki, Y.; Takegawa, N.; Tanimoto, H.; McKenzie, R.; Johnston, P.; Blake, D. R.; Murayama, T.; Koike, M. Formation and transport of oxidized reactive nitrogen, ozone, and secondary organic aerosol in Tokyo. *J. Geophys. Res.* **2008**, *113*, D21310, doi:10.1029/2008JD010134.

(6) Grosjean, E.; Grosjean, D.; Woodhouse, L. F.; Yang, Y. J. Peroxyacetyl nitrate and peroxypropionyl nitrate in Porto Alegre, Brazil. *Atmos. Environ.* **2002**, *36*, 2405–2419.

(7) Wang, T.; Ding, A. J.; Gao, J.; Wu, W. S. Strong ozone production in urban plumes from Beijing, China. *Geophys. Res. Lett.* **2006**, *33*, L01811, doi:10.1029/2005GL024975.

(8) Zhao, C.; Wang, Y. H.; Zeng, T. East China Plains: A "Basin" of Ozone Pollution. *Environ. Sci. Technol.* **2009**, *43*, 1911–1915.

(9) Zhang, Y. H.; Su, H.; Zhong, L. J.; Cheng, Y. F.; Zeng, L. M.; Wang, X. S.; Xiang, Y. R.; Wang, J. L.; Gao, D. F.; Shao, M.; Fan, S. J.; Liu, S. C. Regional ozone pollution and observation-based approach for analyzing ozone-precursor relationship during the PRIDE-PRD2004 campaign. *Atmos. Environ.* **2008**, *42*, 6203–6218.

(10) Chou, C. C. K.; Tsai, C. Y.; Shiu, C. J.; Liu, S. C.; Zhu, T. Measurement of NO_y during Campaign of Air Quality Research in Beijing 2006 (CAREBeijing-2006): Implications for the ozone production efficiency of NO_x. *J. Geophys. Res.* **2009**, *114*, D00G01, doi:10.1029/2008JD010446.

(11) Shao, M.; Lu, S. H.; Liu, Y.; Xie, X.; Chang, C. C.; Huang, S.; Chen, Z. M. Volatile organic compounds measured in summer in Beijing and their role in ground-level ozone formation. *J. Geophys. Res.* **2009**, *114*, D00G06, doi:10.1029/2008JD010863.

(12) Hofzumahaus, A.; Rohrer, F.; Lu, K. D.; Bohn, B.; Brauers, T.; Chang, C. C.; Fuchs, H.; Holland, F.; Kita, K.; Kondo, Y.; Li, X.; Lou, S. R.; Shao, M.; Zeng, L. M.; Wahner, A.; Zhang, Y. H. Amplified Trace Gas Removal in the Troposphere. *Science* **2009**, *324*, 1702–1704.

(13) Lu, K. D.; Zhang, Y. H.; Su, H.; Brauers, T.; Chou, C. C.; Hofzumahaus, A.; Liu, S. C.; Kita, K.; Kleffmann, J.; Kondo, Y.; Shao, M.; Wahner, A.; Wang, J. L.; Wang, X. S.; Wiesen, P.; Zhu, T. Oxidant (O_3+NO_2) production processes and formation regimes in Beijing. *J. Geophys. Res.* **2010**, *115*, D07303, doi:10.1029/2009JD01271.

(14) Grosjean, D. Ambient PAN and PPN in southern California from 1960 to the SCOS97-NARSTO. *Atmos. Environ.* **2003**, *37*, S221–S238.

(15) Marley, N. A.; Gaffney, J. S.; Ramos-Villegas, R.; Gonzalez, B. C. Comparison of measurements of peroxyacyl nitrates and primary carbonaceous aerosol concentrations in Mexico City determined in 1997 and 2003. *Atmos. Chem. Phys.* **2007**, *7*, 2277–2285.

(16) Zhang, J. M.; Wang, T.; Ding, A. J.; Zhou, X. H.; Xue, L. K.; Poon, C. N.; Wu, W. S.; Gao, J.; Zuo, H. C.; Chen, J. M.; Zhang, X. C.; Fan, S. J. Continuous measurement of peroxyacetyl nitrate (PAN) in suburban and remote areas of western China. *Atmos. Environ.* **2009**, *43*, 228–237.

(17) Zhang, X.; Chen, Z. M.; He, S. Z.; Hua, W.; Zhao, Y.; Li, J. L. Peroxyacetic acid in urban and rural atmosphere: concentration, feedback on PAN-NOx cycle and implication on radical chemistry. *Atmos. Chem. Phys.* **2010**, *10*, 737–748.

(18) Ryerson, T. B.; Williams, E. J.; Fehsenfeld, F. C. An efficient photolysis system for fast-response NO_2 measurements. *J. Geophys. Res.* **2000**, *105*, 26447–26461.

(19) Slusher, D. L.; Huey, L. G.; Tanner, D. J.; Flocke, F. M.; Roberts, J. M. A thermal dissociation-chemical ionization mass spectrometry (TD-CIMS) technique for the simultaneous measurement of peroxyacyl nitrates and dinitrogen pentoxide. *J. Geophys. Res.* **2004**, *109*, D19315, doi:10.1029/2004JD004670.

(20) Amoroso, A.; Beine, H. J.; Sparapani, R.; Nardino, M.; Allegrini, I. Observation of coinciding arctic boundary layer ozone depletion and snow surface emissions of nitrous acid. *Atmos. Environ.* **2006**, *40*, 1949–1956.

(21) Amoroso, A.; Beine, H. J.; Esposito, G.; Perrino, C.; Catrambone, M.; Allegrini, I. Seasonal differences in atmospheric nitrous acid near Mediterranean urban areas. *Water, Air, Soil Pollut.* **2008**, *188*, 81–92.

(22) Febo, A.; Perrino, C.; Cortiello, M. A denuder technique for the measurement of nitrous acid in urban atmosphere. *Atmos. Environ.* **1993**, *27A*, 1721–1728.

(23) Ho, S. S. H.; Yu, J. Z. Determination of airborne carbonyls: Comparison of a thermal desorption/GC method with the standard DNPH/HPLC method. *Environ. Sci. Technol.* **2004**, *38*, 862–870.

(24) Choi, Y.; Wang, Y. H.; Zeng, T.; Martin, R. V.; Kurosu, T. P.; Chance, K. Evidence of lightning NO_x and convective transport of pollutants in satellite observations over North America. *Geophys. Res. Lett.* **2005**, *32*, L02805, doi:10.1029/2004GL021436.

(25) Choi, Y.; Wang, Y. H.; Zeng, T.; Cunnold, D.; Yang, E. S.; Martin, R.; Chance, K.; Thouret, V.; Edgerton, E. Springtime transitions of NO_2, CO, and O_3 over North America: Model evaluation and analysis. *J. Geophys. Res.* **2008**, *113*, D20311, doi:10.1029/2007JD009632.

(26) Choi, Y.; Wang, Y. H.; Yang, Q.; Cunnold, D.; Zeng, T.; Shim, C.; Luo, M.; Eldering, A.; Bucsela, E.; Gleason, J. Spring to summer northward migration of high O_3 over the western North Atlantic. *Geophys. Res. Lett.* **2008**, *35*, L04818, doi:10.1029/2007GL032276.

(27) Wang, Y. H.; Choi, Y.; Zeng, T.; Davis, D.; Buhr, M.; Huey, L. G.; Neff, W. Assessing the photochemical impact of snow NO_x emissions over Antarctica during ANTCI 2003. *Atmos. Environ.* **2007**, *41*, 3944–3958.

(28) Zhao, C.; Wang, Y. H. Assimilated inversion of NO_x emissions over east Asia using OMI NO_2 column measurements. *Geophys. Res. Lett.* **2009**, *36*, L06805, doi:10.1029/2008GL037123.

(29) Zhao, C.; Wang, Y. H.; Choi, Y.; Zeng, T. Summertime impact of convective transport and lightning NOx production over North America: modeling dependence on meteorological simulations. *Atmos. Chem. Phys.* **2009**, *9*, 4315–4327.

(30) Zhao, C.; Wang, Y.; Yang, Q.; Fu, R.; Cunnold, D.; Choi, Y. Impact of East Asian summer monsoon on air quality over China: The view from space. *J. Geophys. Res.* **2010**, *115*, D09301 (doi: 10.1029/2009JD012745).

(31) Sander, S. P.; Friedl, R. R.; Golden, D. M.; Kurylo, M. J.; Moortgat, G. K.; Keller-Rudek, H.; Wine, P. H.; Ravishankara, A. R.; Kolb, C. E.; Molina, M. J.; Finlayson-Pitts, B. J.; Huie, R. E.; Orkin, V. L. *Chemical kinetics and photochemical data for use in atmospheric studies*; Evaluation Number 15, JPL Publication 06-02; Jet Propulsion Laboratory: Pasadena, CA, USA, 2006.

(32) Carter, W. P. L. Development of the SAPRC-07 chemical mechanism and upadated ozone reactivity scales; Final Report to the California Air Resources Board Contract No. 03-318; 2009.

(33) Luke, W. T.; Kelley, P.; Lefer, B. L.; Flynn, J.; Rappenglück, B.; Leuchner, M.; Dibb, J. E.; Ziemba, L. D.; Anderson, C. H.; Buhr, M. Measurements of primary trace gases and NO_y composition in Houston, Texas. *Atmos. Environ.* **2009** (doi:10.1016/j.atmosenv.2009.08.014).

(34) Kanaya, Y.; Cao, R. Q.; Akimoto, H.; Fukuda, M.; Komazaki, Y.; Yokouchi, Y.; Koike, M.; Tanimoto, H.; Takegawa, N.; Kondo, Y. Urban photochemistry in central Tokyo: 1. Observed and modeled OH and HO_2 radical concentrations during the winter and summer of 2004. *J. Geophys. Res.* **2007**, *112*, D21312, doi:10.1029/2007JD008670.

(35) Elshorbany, Y. F.; Kurtenbach, R.; Wiesen, P.; Lissi, E.; Rubio, M.; Villena, G.; Gramsch, E.; Rickard, A. R.; Pilling, M. J.; Kleffmann, J. Oxidation capacity of the city air of Santiago, Chile. *Atmos. Chem. Phys.* **2009**, *9*, 2257–2273.

(36) Gerecke, A.; Thielmann, A.; Gutzwiller, L.; Rossi, M. J. The chemical kinetics of HONO formation resulting from heterogeneous interaction of NO_2 with flame soot. *Geophys. Res. Lett.* **1998**, *25*, 2453–2456.
(37) Kleffmann, J. Daytime Sources of Nitrous Acid (HONO) in the Atmospheric Boundary Layer. *Chem. Phys. Chem.* **2007**, *8*, 1137–1144.
(38) Bey, I.; Jacob, D. J.; Yantosca, R. M.; Logan, J. A.; Field, B. D.; Fiore, A. M.; Li, Q. B.; Liu, H. G. Y.; Mickley, L. J.; Schultz, M. G. Global modeling of tropospheric chemistry with assimilated meteorology: Model description and evaluation. *J. Geophys. Res.* **2001**, *106*, 23073–23095.
(39) Mao, T.; Wang, Y. S.; Jiang, J.; Wu, F. K.; Wang, M. X. The vertical distributions of VOCs in the atmosphere of Beijing in autumn. *Sci. Total Environ.* **2008**, *390*, 97–108.
(40) Song, Y.; Shao, M.; Liu, Y.; Lu, S. H.; Kuster, W.; Goldan, P.; Xie, S. D. Source apportionment of ambient volatile organic compounds in Beijing. *Environ. Sci. Technol.* **2007**, *41*, 4348–4353.
(41) Wang, X. M.; Sheng, G. Y.; Fu, J. M.; Chan, C. Y.; Lee, S. G.; Chan, L. Y.; Wang, Z. S. Urban roadside aromatic hydrocarbons in three cities of the Pearl River Delta, People's Republic of China. *Atmos. Environ.* **2002**, *36*, 5141–5148.
(42) Zhang, J.; Wang, T.; Chameides, W. L.; Cardelino, C.; Kwok, J.; Blake, D. R.; Ding, A.; So, K. L. Ozone production and hydrocarbon reactivity in Hong Kong, Southern China. *Atmos. Chem. Phys.* **2007**, *7*, 557–573.
(43) Ran, L.; Zhao, C. S.; Geng, F. H.; Tie, X. X.; Tang, X.; Peng, L.; Zhou, G. Q.; Yu, Q.; Xu, J. M.; Guenther, A. Ozone photochemical production in urban Shanghai, China: Analysis based on ground level observations. *J. Geophys. Res.* **2009**, *114*, D15301, doi: 10.1029/2008JD010752.
(44) Emmerson, K. M.; Evans, M. J. Comparison of tropospheric gas-phase chemistry schemes for use within global models. *Atmos. Chem. Phys.* **2009**, *9*, 1831–1845.
(45) Wang, Y. X.; McElroy, M. B.; Munger, J. W.; Hao, J.; Ma, H.; Nielsen, C. P.; Chen, Y. Variations of O_3 and CO in summertime at a rural site near Beijing. *Atmos. Chem. Phys.* **2008**, *8*, 6355–6363.
(46) Zhang, Q.; Streets, D. G.; Carmichael, G. R.; He, K. B.; Huo, H.; Kannari, A.; Klimont, Z.; Park, I. S.; Reddy, S.; Fu, J. S.; Chen, D.; Duan, L.; Lei, Y.; Wang, I. T.; Yao, Z. L. Asian emissions in 2006 for the NASA INTEX-B mission. *Atmos. Chem. Phys.* **2009**, *9*, 5131–5153.
(47) Bloss, C.; Wagner, C.; Bonzanini, A.; Jenkin, M. E.; Wirtz, K.; Martin-Reviejo, M.; Pilling, M. J. Evaluation of detailed aromatic mechanisms (MCMv3 and MCMv3.1) against environmental chamber data. *Atmos. Chem. Phys.* **2005**, *5*, 623–639.

ES1007966